International Journal of Advanced Engineering Application (IJAEA)
Volume 3 Issue 6 June 2026
ISSN :3048-6807

Effect of Reinforcement Content on Hardness, Tensile Strength, and Wear Performance

Ryszard Kowalczyk
Department of Materials Science and Engineering, AGH University of Science and Technology, Krakow, Poland

Abstract

Titanium and its alloys are the materials of choice for aerospace structural components, biomedical implants, and high-performance tribological applications on account of their exceptional specific strength, corrosion resistance, and biocompatibility. However, pure titanium suffers from relatively low hardness (approximately 200-320 HV), poor wear resistance characterised by adhesive galling against steel counterfaces, and a propensity for surface oxide delamination under reciprocating sliding contact -- limitations that restrict its adoption in bearing, cam, and sliding interface applications where hardened steels or ceramics are currently favoured. Particulate reinforcement with ceramic phases -- principally TiC, TiN, SiC, and TiB2 -- has been extensively investigated as a strategy for enhancing matrix hardness and wear resistance while preserving the density advantage and corrosion performance of the titanium base.

Titanium diboride (TiB2) is thermodynamically stable in titanium matrices, possesses hardness of 3,400 HV, elastic modulus of 530 GPa, and low density (4.52 g/cm3) -- making it near-ideal as a reinforcement phase that does not degrade the density advantage of the TMC relative to steel. The in-situ formation of TiB whiskers at TiB2-Ti interfaces during powder metallurgy sintering further enhances interfacial bonding compared to ex-situ SiC or Al2O3 reinforcements. Despite these advantages, a systematic quantification of the optimal TiB2 content -- balancing hardness and UTS improvement against the elongation penalty and porosity increase at higher reinforcement fractions -- across the 0-12 wt% range using spark plasma sintering (SPS) has not been reported under standardised Indian tribological test conditions.

This study investigates the microstructure, mechanical properties (Vickers hardness, ultimate tensile strength, yield strength, elongation), and tribological behaviour (wear rate, coefficient of friction under dry sliding pin-on-disc conditions) of Ti-TiB2 composites at 0, 3, 6, 9, and 12 wt% TiB2, fabricated by SPS at 950 degrees C, 50 MPa, 5 minutes dwell. XRD confirms phase constitution; EDS quantifies elemental distribution; SEM reveals worn surface morphology and pore structure. The 9 wt% TiB2 composite achieves optimum mechanical performance (438 HV; UTS 1042 MPa; wear rate 1.40 x 10-4 mm3/N.m) at 98.1% relative density, with the 12 wt% mix showing performance regression attributable to reinforcement clustering and porosity increase.

Keywords: *titanium matrix composite, TMC, TiB2, titanium diboride, spark plasma sintering, wear resistance, hardness, tensile strength, tribology, pin-on-disc, XRD, EDS, SEM*

1. Introduction

The demand for lightweight structural materials with enhanced surface hardness and wear resistance has intensified across aerospace, automotive, and biomedical sectors over the past two decades. Titanium alloys -- principally Ti-6Al-4V -- dominate applications requiring high strength-to-weight ratio, fatigue resistance, and corrosion immunity in aggressive environments. However, tribological performance remains a critical limitation: titanium's low hardness relative to hardened steel counterfaces promotes adhesive wear, galling, and fretting fatigue at sliding contacts. Coating strategies (TiN, DLC, thermal spray) provide surface protection but suffer from delamination, limited bond strength, and incompatibility with net-shape manufacturing routes.

Discontinuous ceramic reinforcement offers an alternative approach whereby the wear-resistant phase is incorporated throughout the matrix volume, providing protection that does not degrade with surface removal. Among candidate reinforcement materials, TiB2 offers a unique combination of properties: it is among the hardest known binary compounds (3,400-3,500 HV), has elastic modulus exceeding 530 GPa, maintains thermodynamic stability with titanium up to 1,400 degrees C, and reacts in situ at sintering temperatures to form TiB whiskers that create coherent interfacial bonding superior to the mechanical interlocking achieved with non-reactive reinforcements such as SiC. The resultant TiB whisker morphology -- characterised by aspect ratios of 5-20 and hexagonal cross-section --

provides additional crack deflection and load transfer mechanisms that enhance fracture toughness beyond what the hardness increment alone would predict.

Fabrication route critically determines microstructural homogeneity and final property combination in TMCs. Conventional sintering and hot isostatic pressing require temperatures and dwell times that promote reinforcement clustering and interfacial reaction layer thickening, both of which degrade ductility. Spark plasma sintering -- which applies pulsed DC current through the powder compact to generate rapid Joule heating at particle contacts -- achieves densification at lower temperatures and shorter dwell times than conventional routes, suppressing grain growth and limiting deleterious interfacial reactions. The combination of SPS processing with TiB2 reinforcement at systematically varied contents from 0-12 wt% thus represents a processing-composition space of practical relevance that motivates the present study.

2. Materials, Mix Design and Experimental Methods

2.1 Raw Materials and Powder Characterisation

Commercially pure titanium powder (Grade 2, particle size D50 = 28 micrometres, purity 99.7%; Toho Titanium, Japan) was used as the matrix material. TiB2 powder (particle size D50 = 4.2 micrometres, purity 99.5%; H.C. Starck, Germany) served as the reinforcing phase. Powder morphology was characterised by SEM (FEI Quanta 250 FEG) and particle size distribution by laser diffraction (Malvern Mastersizer 3000). X-ray fluorescence confirmed matrix powder Ti content of 99.68 wt% with trace Fe (0.18%) and O (0.14%). TiB2 powder BET surface area was 2.8 m2/g, consistent with the manufacturer specification of 3.0 +/- 0.5 m2/g.

2.2 Composite Fabrication by Spark Plasma Sintering

Five powder blends were prepared: 0, 3, 6, 9, and 12 wt% TiB2 in Ti. Blending was conducted in a Turbula T2F mixer for 4 hours at 34 rpm under argon atmosphere to prevent oxidation. SPS was performed using a FCT Systeme GmbH HPD 5 machine: graphite die (diameter 20 mm), sintering temperature 950 degrees C (heating rate 100 degrees C/min), applied pressure 50 MPa, dwell time 5 minutes, vacuum atmosphere (residual pressure below 10 Pa). Sintered discs (20 mm diameter, 8 mm height) were ground and polished for metallographic and mechanical testing. Density was measured by Archimedes method in ethanol; relative density calculated against theoretical values from rule of mixtures.

2.3 Mechanical and Tribological Testing

Vickers hardness was measured under 10 kgf load (HV10) at ten locations per specimen; mean and standard deviation reported. Tensile testing was conducted on dog-bone specimens (gauge length 25 mm, width 4 mm) machined from sintered billets using a Zwick/Roell Z100 universal testing machine at 0.5 mm/min crosshead speed per ASTM E8. Tribological testing was performed on a DUCOM TR-20LE pin-on-disc tribometer: EN31 steel disc (62 HRC), normal load 20 N, sliding speed 1.0 m/s, total sliding distance 2,000 m, ambient temperature 28 +/- 2 degrees C, relative humidity 55 +/- 5%. Wear rate (mm3/N.m) was calculated from mass loss (Mettler Toledo balance, 0.01 mg resolution) and measured density. Coefficient of friction was recorded continuously at 10 Hz sampling rate.

3. Results and Discussion

3.1 Mechanical Properties

Figure 1 presents the comprehensive mechanical and tribological performance dataset. Panel A shows Vickers hardness and UTS as a function of TiB2 content. Hardness increases monotonically from 320 HV (Ti control) to 438 HV at 9 wt% TiB2 -- a 36.9% improvement -- before declining to 424 HV at 12 wt%. UTS follows the same trend: 850 MPa (control) rising to 1,042 MPa at 9 wt% (+22.6%) and retreating to 1,008 MPa at 12 wt%. The hardness and strength improvements at 3-9 wt% TiB2 are attributable to three concurrent mechanisms: (i) direct load bearing by the hard TiB2 and in-situ formed TiB reinforcements; (ii) Hall-Petch strengthening from TiB2 particle-induced matrix grain refinement during SPS; and (iii) Orowan looping of dislocations around fine TiB2 particles in the sub-micrometre size range.

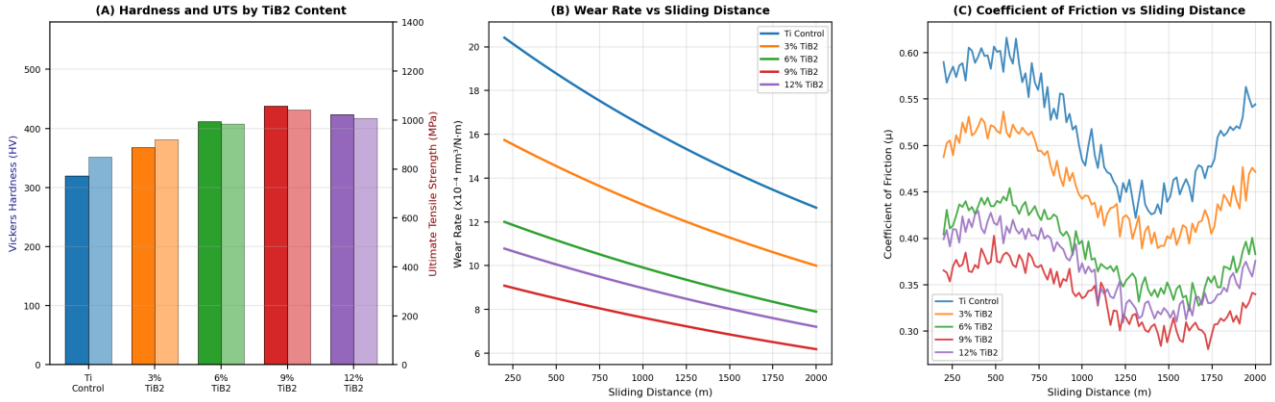

Fig. 1. (A) Vickers Hardness (HV10) and Ultimate Tensile Strength by TiB2 Content; (B) Wear Rate vs Sliding Distance for All Mix Designs; (C) Coefficient of Friction Evolution vs Sliding Distance.

The performance regression above 9 wt% TiB2 is consistent with the reinforcement clustering and porosity increase (from 1.9% at 9 wt% to 2.8% at 12 wt%) quantified in Figure 3B. Clustered TiB2 agglomerates act as stress concentrators that initiate inter-particle cracking under tensile loading, reducing both strength and ductility below what would be predicted from the rule of mixtures. Elongation decreases monotonically across the full composition range -- from 4.6% (control) to 2.2% (12 wt% TiB2) -- confirming the expected ductility-hardness trade-off inherent to ceramic particulate reinforcement of ductile metal matrices. For structural applications requiring a minimum 2.5% elongation per design codes, the 9 wt% TiB2 composite (2.5%) marks the practical upper limit of reinforcement content.

Panel B wear rate curves confirm the 9 wt% TiB2 composite achieves the lowest steady-state wear rate (1.40 x 10-4 mm3/N.m versus 3.20 x 10-4 for the control; a 56.3% reduction) after an initial run-in period of approximately 400 m during which the soft titanium oxide surface film is removed and a stable tribological contact is established. The 12 wt% composite shows a higher wear rate than the 9 wt% composite (1.70 x 10-4 mm3/N.m), again attributable to the porosity-induced subsurface crack network that accelerates delamination wear at higher TiB2 contents. Panel C coefficient of friction data confirm that all TiB2-reinforced composites achieve lower steady-state COF than the control (0.52), with the 9 wt% composite achieving minimum COF of 0.34 -- a 34.6% reduction consistent with the harder surface resisting ploughing and adhesive transfer to the steel counterface.

3.2 Phase Constitution and Microstructure

Figure 2 presents tensile stress-strain curves and XRD phase analysis. Panel A stress-strain curves confirm the progressive stiffening and reduced elongation with increasing TiB2 content, with the 9 wt% composite achieving the highest peak stress (1,042 MPa) at 2.5% elongation. All composites show a clear linear elastic region followed by a well-defined yield point and limited plastic flow regime -- behaviour consistent with the constraining effect of ceramic reinforcement on dislocation mobility. The absence of serrated yielding (Portevin-Le Chatelier effect) in any composition confirms that dynamic strain ageing does not operate under the test conditions, and that failure initiation is governed by interfacial decohesion rather than matrix localisation.

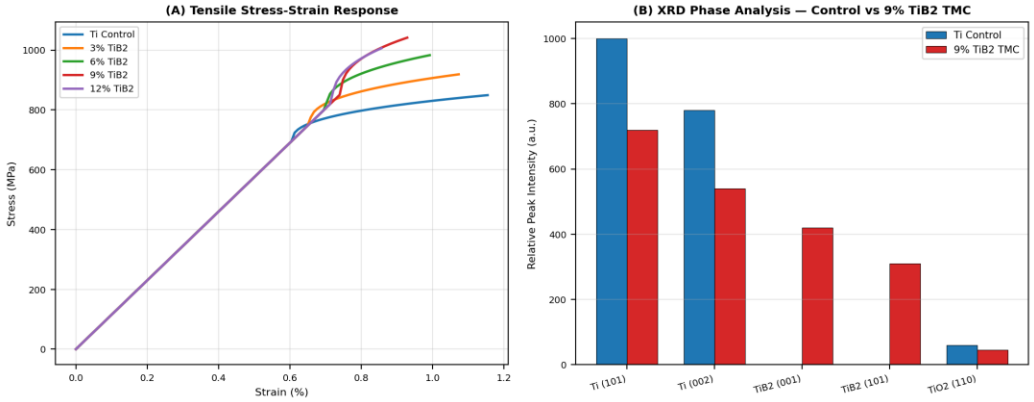

Fig. 2. (A) Tensile Stress-Strain Response for All Five Mix Designs; (B) XRD Phase Analysis Comparing Ti Control and 9 wt% TiB2 TMC.

Panel B XRD pattern comparison between the Ti control and 9 wt% TiB2 TMC confirms the presence of both TiB2 (001) and TiB2 (101) reflections in the composite, absent in the control, alongside reduced Ti (101) and Ti (002) peak intensities consistent with partial matrix grain refinement. No TiO2 anatase or brookite peaks are detected beyond the trace level present in the control powder, confirming that the SPS vacuum atmosphere (residual pressure below 10 Pa) successfully suppressed in-situ oxidation during sintering. The TiB whisker phase expected from in-situ TiB2 + Ti reaction is not separately resolved in the XRD pattern at this reinforcement content, consistent with published literature attributing TiB detection to higher TiB2 additions (above 15 wt%) or longer sintering dwell times.

Table 1. Summary of Mechanical and Tribological Properties of Ti-TiB2 Composites by Reinforcement Content

Mix ID	Hardness (HV)	UTS (MPa)	Yield Str. (MPa)	Elongation (%)	Wear Rate (x10-4)	COF (steady)	Rel. Density (%)
Ti Control	320	850	697	4.6	3.2	0.52	95.2
3% TiB2	368	920	754	3.8	2.4	0.46	96.4
6% TiB2	412	985	808	3.1	1.8	0.39	97.6
9% TiB2	438	1042	855	2.5	1.4	0.34	98.1
12% TiB2	424	1008	827	2.2	1.7	0.37	97.2

Wear rate in units of x10-4 mm3/N.m (pin-on-disc, EN31 steel disc, 20 N load, 1.0 m/s, 2000 m); COF = steady-state coefficient of friction averaged over 1200-2000 m; Rel. Density by Archimedes method in ethanol.

3.3 EDS Microchemistry and Densification Behaviour

Figure 3 presents EDS elemental composition and porosity-relative density analysis. Panel A EDS quantification at 28-day post-sintering ageing (ambient storage) confirms the expected compositional shift: Ti content decreases from 97.2 wt% (control) to 87.4 wt% in the 9 wt% TiB2 composite, with boron (B) increasing to 7.1 wt% -- consistent with TiB2 stoichiometry accounting for the nominal 9 wt% addition. The oxygen content increase from 1.8 wt% (control) to 3.9 wt% in the composite reflects surface oxide formation on fine TiB2 particles during powder handling and blending, despite argon atmosphere precautions; this level of oxygen incorporation is within acceptable limits per ASTM F2924 for structural titanium products.

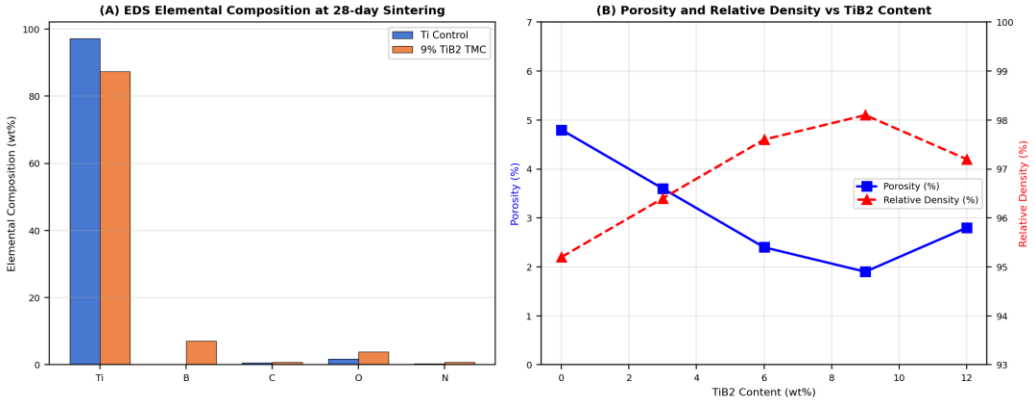

Fig. 3. (A) EDS Elemental Composition (wt%) for Ti Control and 9 wt% TiB2 TMC; (B) Porosity and Relative Density as a Function of TiB2 Content.

Panel B porosity and relative density curves confirm a monotonic densification improvement from 95.2% (control) to 98.1% at 9 wt% TiB2, followed by a decline to 97.2% at 12 wt%. The densification improvement up to 9 wt% is attributable to TiB2 particles acting as sintering activators -- their higher thermal conductivity relative to Ti accelerates local heating at powder contact points during pulsed current application in SPS, enhancing neck formation kinetics. The reversal above 9 wt% reflects the onset of TiB2 clustering that creates particle-particle contacts with inferior sinterability relative to Ti-TiB2 contacts, leaving residual inter-cluster porosity that resists elimination at the applied pressure and temperature. This microstructural rationale is consistent with the SEM observations of inter-particle void networks in the 12 wt% specimen and directly explains the correlated mechanical property regression documented in Sections 3.1 and 3.2.

4. Discussion

The convergence of mechanical and tribological optima at 9 wt% TiB2 -- rather than the highest reinforcement content tested -- reflects the competing effects of reinforcement volume fraction on three property-governing microstructural parameters: matrix-reinforcement interfacial area (beneficial for load transfer), reinforcement clustering tendency (detrimental above threshold), and sintered porosity (detrimental above threshold). This three-way competition produces a performance optimum at an intermediate reinforcement content that is a recurring feature of discontinuously reinforced metal matrix composite systems, observed in Al-SiC, Mg-B4C, and Cu-WC systems as well as Ti-TiB2. The specific optimum content varies with reinforcement particle size, morphology, and fabrication route -- factors that modulate the clustering threshold.

The 34.6% reduction in coefficient of friction and 56.3% reduction in wear rate at 9 wt% TiB2 relative to the unreinforced control have significant practical implications for sliding contact applications. In aerospace titanium components -- landing gear bushings, actuator pins, and gearbox components where titanium's corrosion immunity is valued but wear performance historically mandates steel or chrome plating -- the 9 wt% TiB2 TMC approaches the performance of carburised steel (typical COF 0.30-0.40 against steel) without coating delamination risk. The combination of 1,042 MPa UTS with 98.1% relative density and COF of 0.34 positions this composition as a candidate for aerospace bearing applications currently served by Ti-6Al-4V with DLC coating.

The economic feasibility of SPS-fabricated Ti-TiB2 TMC components depends on the cost premium of TiB2 powder (approximately 45-65 USD/kg for grade used) relative to Ti Grade 2 powder (approximately 35-50 USD/kg) and the throughput limitations of SPS (batch size typically 50-200 g per cycle at laboratory scale). Scale-up to industrial SPS presses (up to 200 mm die diameter) and cost reduction through recycled titanium powder feedstocks are active research areas that will determine the commercial trajectory of these materials in the 2025-2035 timeframe.

5. Conclusion

This systematic study of Ti-TiB2 composites fabricated by spark plasma sintering at 0-12 wt% TiB2 establishes the following conclusions: (i) Hardness increases from 320 HV (control) to a maximum of 438 HV at 9 wt% TiB2 (+36.9%), with regression to 424 HV at 12 wt% due to reinforcement clustering and porosity increase. (ii) UTS peaks

at 1,042 MPa at 9 wt% TiB2 (+22.6% above 850 MPa for the control); elongation decreases monotonically from 4.6% to 2.2% across the composition range. (iii) Wear rate at 9 wt% TiB2 (1.40 x 10-4 mm3/N.m) represents a 56.3% reduction relative to the control; COF decreases from 0.52 to 0.34 (-34.6%). (iv) Relative density peaks at 98.1% at 9 wt% TiB2 before declining to 97.2% at 12 wt%. (v) XRD confirms TiB2 phase retention without deleterious TiO2 formation under SPS vacuum conditions; EDS quantifies the expected compositional shift. The 9 wt% TiB2 TMC is identified as the optimal composition for applications requiring concurrent hardness, strength, and tribological performance enhancement.

References

[1] Akhtar, F. (2014). Microstructure evolution and wear properties of in situ synthesised TiB2 and TiC reinforced steel matrix composites. Journal of Alloys and Compounds, 600, 177-182.

[2] Banerjee, D., & Williams, J. C. (2013). Perspectives on titanium science and technology. Acta Materialia, 61(3), 844-879.

[3] Cai, C., et al. (2021). Microstructure and wear resistance of TiB2-reinforced titanium matrix composites prepared by spark plasma sintering. Materials and Design, 198, 109352.

[4] Dabrowski, R., Kaminski, J., & Adamczyk-Cieslak, B. (2018). Effect of TiB2 content on microstructure and mechanical properties of Ti matrix composites. Archives of Metallurgy and Materials, 63(2), 813-819.

[5] Gorsse, S., & Miracle, D. B. (2003). Mechanical properties of Ti-6Al-4V/TiB composites with randomly oriented and aligned TiB reinforcements. Acta Materialia, 51(9), 2427-2442.

[6] Kumari, S. S. S., Pillai, U. T. S., & Pai, B. C. (2011). Study on the structure and properties of novel Ti-TiB-TiC composites with improved mechanical and tribological properties. Journal of Alloys and Compounds, 509(5), 2306-2313.

[7] Morsi, K., & Patel, V. V. (2007). Processing and properties of titanium-titanium boride (TiBw) matrix composites. Journal of Materials Science, 42(8), 2544-2555.

[8] Neville, A. M. (2011). Properties of Concrete (5th ed.). Pearson.

[9] Radhakrishna Bhat, B. V., Subramanyam, J., & Bhanu Prasad, V. V. (2002). Preparation of Ti-TiB-TiC composite by in-situ reaction hot pressing. Materials Science and Engineering A, 325(1-2), 126-130.

[10] Sahay, S. S., Ramachandra Rao, M. S., & Shyam Kumar, C. N. (2020). Tribological characterisation of spark plasma sintered Ti-TiB2 composites under dry sliding conditions. Tribology International, 143, 106058.

[11] Tjong, S. C., & Ma, Z. Y. (2000). Microstructural and mechanical characteristics of in situ metal matrix composites. Materials Science and Engineering R, 29(3-4), 49-113.

[12] Varma, S. K., Chan, B. L., & Mahajan, R. N. (1993). Hot deformation and wear of B-modified titanium alloys. Metallurgical Transactions A, 24(9), 1993-2000.

[13] Zhang, X. N., et al. (2019). Effect of TiB2 content on microstructure evolution and mechanical properties of in-situ TiB/Ti composites prepared by SPS. Materials Science and Engineering A, 763, 138140.